JOURNAL OF MAGNETIC RESONANCE **132,** 102–108 (1998)
ARTICLE NO. MN981394

Is the sech/tanh Adiabatic Pulse Really Adiabatic?

Daniel Rosenfeld*,[1] and Yuval Zur†

*School of Physics and Astronomy, Tel-Aviv University, Tel-Aviv 69978, Israel; and †Elscint MRI Center, P.O. Box 550, Haifa 31004, Israel

Received August 18, 1997; revised December 31, 1997

Adiabatic pulses are most conveniently studied in the frequency frame which is a frame of reference rotating at the instantaneous frequency of the pulse. In this frame the adiabatic condition $\|\gamma \mathbf{B}_{\mathbf{eff}}\| \gg |\dot{\theta}|$ sets an upper limit on the sweep rate $\dot{\theta}$ of the $\mathbf{B}_{\mathbf{eff}}$ vector. This, in turn, places a lower bound on the pulse duration. Adiabatic behavior is studied at the threshold duration and two pulses are examined: (i) a pulse with a constant sweep rate (CAP pulse) and (ii) a conventional sech/tanh adiabatic pulse. It is shown that the sech/tanh pulse performs robust magnetization inversion although it seems to violate the adiabatic condition. This puzzling phenomenon is solved by switching into a second-order rotating frame of reference (SORF) where it is shown that the adiabatic condition is fulfilled. This frame coincides with the frequency frame at the beginning of the pulse. Assuming an RF field along the *x*-axis of the frequency frame, the SORF then rotates about the common *y*-axis during the pulse with the *z*-axis of the new frame aligned with the $\mathbf{B}_{\mathbf{eff}}$ vector. It is shown that adiabatic motion may be performed in the SORF, in which the sweep rate is increased indefinitely; the adiabatic condition is violated by this motion in the frequency frame but is fulfilled in the SORF. The lower bound on the sweep rate in the frequency frame is thereby lifted.

Adiabatic fast passage has long been used to invert a selected band of spins. These pulses retain their robustness even when subjected to nonuniform RF amplitude. The pulse is defined by its instantaneous amplitude $\omega_1(t) = \gamma B_1(t)$ and frequency $\omega(t)$ and is most conveniently studied in the *frequency frame,* which is a frame of reference rotating at the instantaneous frequency of the pulse (*1*). It operates by causing the magnetization vector $\mathbf{M}$ to follow the effective field vector $\boldsymbol{\omega}_e = \gamma \mathbf{B}_{\text{eff}}$ which is composed of the RF field ω_1 and the resonance offset $\Delta\omega(\omega_0, t) = \omega(t) - \omega_0$, ω_0 being the Larmor frequency of the spin we are inspecting. The *adiabatic theorem* (*2*) asserts that the magnetization vector $\mathbf{M}$ remains spin-locked to $\boldsymbol{\omega}_e$ provided that the rate of precession of $\mathbf{M}$ about $\boldsymbol{\omega}_e$ is much faster than the angular velocity of the motion of $\boldsymbol{\omega}_e$. Mathematically this is expressed by the *adiabatic condition* (*3*),

$$Q(\omega_0, t) \gg 1, \qquad [1]$$

where Q is the adiabatic parameter,

$$Q(\omega_0, t) = \frac{\|\boldsymbol{\omega}_e(\omega_0, t)\|}{|\dot{\theta}(\omega_0, t)|}, \qquad [2]$$

and $\tan\theta = \Delta\omega/\omega_1$. Inversion is obtained when the effective field moves the longitudinal magnetization M_z from the $+z$ to the $-z$ axis over a wide band of Larmor frequencies.

We confine ourselves hereafter to on-resonance behavior and conveniently define the Larmor frequency at the center of the slice as the zero frequency. Accordingly, ω_0 is omitted from the notation that follows. In the frame of reference of the slice center we may plot the route traced by the tip of the $\boldsymbol{\omega}_e$ vector. This graph of $\boldsymbol{\omega}_1(t)$ vs $\Delta\omega(t)$ is called the *trajectory* of the adiabatic pulse (*4*). An adiabatic pulse is characterized by its trajectory and the rate of motion of $\boldsymbol{\omega}_e$ upon it. Three classic examples (expressed here as amplitude/frequency modulation functions) include the sech/tanh (*5*), sin/cos (*6*), and const/tan (*3*). For a given trajectory, say a half ellipse (*7*) as in the sin/cos and sech/tanh pulses, the adiabatic condition limits the sweep rate $\dot{\theta}$ at which the trajectory is traversed. This, of course, places a lower bound on the pulse duration. We begin by studying this limit more precisely.

For the sake of simplicity we restrict the discussion to trajectories for which the effective field vector has a constant length $\|\boldsymbol{\omega}_e(t)\| = \omega_e \equiv r$. This choice will be further justified later. The adiabatic condition for such pulses is

$$Q(t) = \frac{r}{|\dot{\theta}|} \gg 1. \qquad [3]$$

In order to study the lower limit of this condition it is most intuitive to first examine the simplest motion of the effective field vector.

[1] Address correspondence to: Daniel Rosenfeld, Elscint MRI Center, POB 550 Haifa 31004, Israel. Fax: 972-4-8575-593. E-mail: danny@mri.elscint.co.il.

1090-7807/98 $25.00

Constant Adiabaticity Pulse: In analogy to Ref. (*8*), we define a constant adiabaticity pulse (CAP) as a pulse for which the adiabatic parameter is constant:

$$Q_{\mathrm{CAP}}(t) = q_0. \qquad [4]$$

In our case ω_e = const, which implies that the trajectory is swept at a constant angular velocity with modulation functions

$$\omega_1(t) = r\cos(\pi t/T)$$
$$\Delta\omega(t) = r\sin(\pi t/T). \qquad [5]$$

T is the pulse duration and $t\epsilon\,[-T/2, T/2]$. The pulse duration is, then,

$$T_{\mathrm{CAP}} = \frac{q_0}{r}\,\Theta, \qquad [6]$$

where Θ is the maximal tip angle (e.g., π radians for an inversion pulse), and the constant adiabatic parameter

$$Q_{\mathrm{CAP}} = q_0 = \frac{rT}{\Theta}. \qquad [7]$$

As shown in Refs. (*8–10*), CAP pulses are short and efficient. When q_0 is sufficiently high, that is, when the adiabatic condition is fulfilled, we expect the magnetization vector **M** to remain spin-locked to the field vector $\boldsymbol{\omega}_e$. During the adiabatic following it is anticipated that only a small angle will be extended between the two vectors. When q_0 is too low, on the other hand, the adiabatic condition breaks down and tracking is lost. This causes a large angle to develop between the two vectors.

What is the lowest value of q_0 for which the CAP pulse still inverts the magnetization? The solid line in Fig. 1 shows

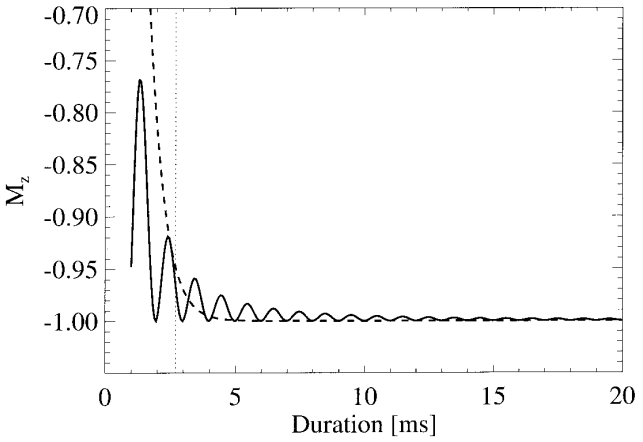

FIG. 1. Final M_z magnetization of a π inversion pulse for different pulse durations for a CAP pulse (solid line) and a sech/tanh pulse (dashed line). The amplitude is $r/2\pi = 1$ kHz. The threshold duration is designated by the dotted vertical line.

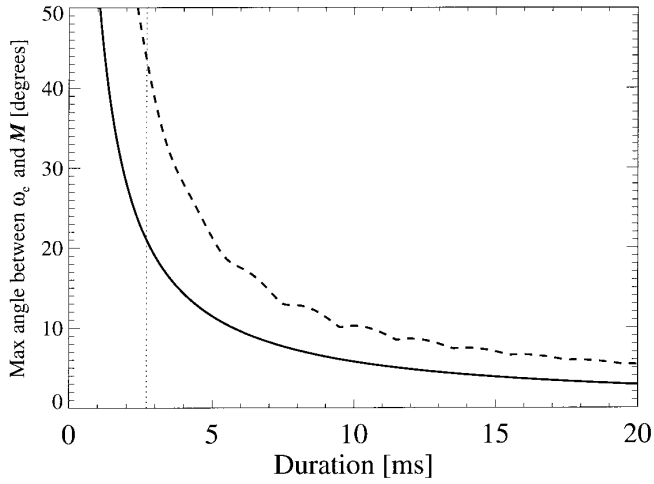

FIG. 2. Maximal angle subtended between the effective field vector $\boldsymbol{\omega}_e$ and the magnetization vector **M** during a π inversion pulse for different pulse durations for a CAP pulse (solid line) and a sech/tanh pulse (dashed line). The amplitude is $r/2\pi = 1$ kHz. The threshold duration is designated by the dotted vertical line.

the final M_z magnetization of a CAP inversion pulse for different pulse durations (cf. Eq. [21] in the Appendix). The amplitude is $r/2\pi = 1$ kHz. The collapse of adiabaticity is apparent in this figure. We chose the threshold duration at $T = 2.7$ ms, which is represented by the vertical dotted line. By Eq. [7] this duration corresponds to the value of $q_0 = 5.4$, that is, inversion is guaranteed when $q_0 \gtrsim 5.4$ [similar results were obtained in Ref. (*8*)].

According to the adiabatic theorem, the better the adiabatic condition is fulfilled, the more the tracking improves. This is demonstrated by the solid line in Fig. 2, where we have plotted the maximal angle subtended between the effective field vector $\boldsymbol{\omega}_e$ and the magnetization vector **M** during the CAP inversion pulse for various pulse durations. It can be seen that at the threshold duration the maximal angle is approximately 21°. At shorter durations the angle increases substantially because tracking is lost.

In summary, the maximal sweep rate of the effective field vector for the CAP pulse is $\dot{\theta} = r/q_0$. By selecting the lowest value for q_0 we achieve the fastest sweep rate and, hence, the shortest pulse.

sech/tanh Adiabatic Pulse: The sech/tanh pulse (*5*) is an efficient adiabatic pulse. Although we are concentrating on on-resonance behavior, it should be mentioned that this pulse is endowed with a robust wideband response. The modulation functions of the sech/tanh pulse are given by (ignoring, for the time being, the assumption of constant r)

$$\omega_1(t) = A\,\mathrm{sech}(\beta t)$$
$$\Delta\omega(t) = B\tanh(\omega t), \qquad [8]$$

where $A = \gamma B_{1\,\max}$ is the peak RF amplitude of the pulse; $B = \mathrm{BW}/2$, where BW is the inverted bandwidth of the pulse; $t \in [-T/2, T/2]$; and $\beta = 10.6/T$ (which ensures truncation of the RF amplitude at 1% of its peak value). We begin by examining the final M_z magnetization on resonance for which there exists an analytic expression (see Ref. (*11*), Eq. [17]):

$$M_z = \begin{cases} -\tanh^2(\pi BT/21.2) + \mathrm{sech}^2(\pi BT/21.2) \\ \quad \times \cos(\pi BT\sqrt{\upsilon^2 - 1}/10.6) \quad \text{for } \upsilon > 1 \\ -\tanh^2(\pi BT/21.2) + \mathrm{sech}^2(\pi BT/21.2) \\ \quad \times \cosh(\pi BT\sqrt{1 - \upsilon^2}/10.6) \quad \text{for } \upsilon \le 1 \end{cases}, \quad [9]$$

where $\upsilon = A/B$. It is interesting to note that although the pulse is defined by three parameters, namely A, B, and T, the actual behavior of M_z is governed by only two dimensionless parameters, the ratio υ and the product BT. In Fig. 3a, contours are plotted of the final M_z magnetization for various values of υ and BT. Inspection of Eq. [9] reveals that for large enough values of BT the leftmost term (i.e., the $\tanh^2$ term) dominates the other, and as a result M_z approaches -1. The thick dashed line in Fig. 3a represents the threshold at which $M_z = -0.95$ [a result similar to the left branch of this curve was obtained by simulation in Ref. (*12*), Fig. 9]; in the blank region above the curve $M_z \le -0.95$ the pulse behaves adiabatically, that is, the pulse continues to invert the magnetization robustly even when A is varied (for fixed values of B and T). In this case υ is treated as a variation parameter which represents the inhomogeneity of B_1 throughout the sample [cf. Refs. (*1, 6, 9*)]. The curve portrays the optimum performance of the sech/tanh pulse; for example, for given values of A and B, the shortest pulse can be read off this graph.

When concerned exclusively with on-resonance performance, one is only limited by the maximum available RF amplitude, viz. $A = \gamma B_{1\,\max}$. For a given value of A, we may

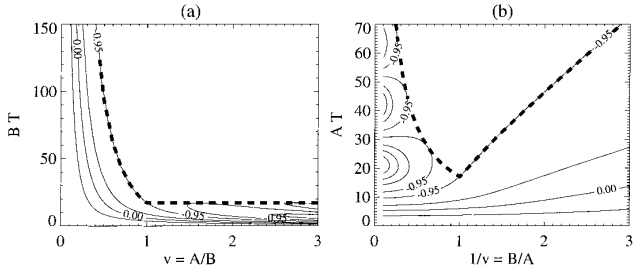

FIG. 3. Contours of the longitudinal magnetization M_z at the end of a sech/tanh pulse plotted (a) for various values of υ and BT (cf. Eq. [9]); (b) for various values of $1/\upsilon$ and AT. The thick dashed line represents the threshold at which $M_z = -0.95$ and the pulse behaves adiabatically; in the blank region above this curve $M_z \le -0.95$.

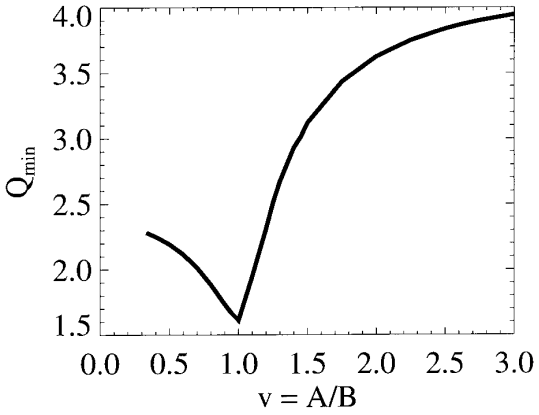

FIG. 4. Minimal value that can be obtained for the adiabatic parameter Q for various values of $\upsilon = A/B$.

then ask what the shortest pulse is which could still achieve inversion. For this purpose, the data in Fig. 3a is more conveniently displayed in the format depicted in Fig. 3b. Here the contours of the final M_z magnetization are plotted for various values of $1/\upsilon = B/A$ and AT. The thick dashed line, which corresponds exactly to the thick dashed line in Fig. 3a, shows clearly that for a given value of A, the shortest inversion pulse is obtained for $B = A$. The pulse duration in this case is $T_{\min} \simeq 17/A$ (for A given in units of rad/s). In particular, in our example for which $A/2\pi = 1$ kHz, the minimal duration is $T_{\min} = 2.7$ ms, which agrees with our choice of the threshold duration.

Next we wish to find the minimal value of the adiabatic parameter Q throughout the pulse. Using $\|\boldsymbol{\omega}_e\| = \sqrt{\omega_1^2 + \Delta\omega^2}$ and $\tan\theta = \Delta\omega/\omega_1$, an expression is obtained for the adiabatic parameter:

$$Q = \frac{\|\boldsymbol{\omega}_e\|}{|\dot{\theta}|} = \frac{1}{10.6}\, BT\, \frac{(\cosh^2\beta t + \upsilon^2 - 1)^{3/2}}{\upsilon \cosh^2\beta t}. \quad [10]$$

The minimal value is obtained by direct derivation of Eq. [10] while keeping in mind that $\cosh \beta t \ge 1$. Some straightforward algebra yields

$$Q_{\min} = \begin{cases} \dfrac{3\sqrt{3}}{21.2}\, BT\, \dfrac{\sqrt{\upsilon^2 - 1}}{\upsilon} & \text{for } \upsilon > \sqrt{3/2} \\ BT\upsilon^2/10.6 & \text{for } \upsilon \le \sqrt{3/2} \end{cases}. \quad [11]$$

It is interesting to note that like M_z in Eq. [9], $Q_{\min}$ is also a function of the two parameters υ and BT. Now, for each value of υ, the minimal BT is given by the thick dashed line in Fig. 3a. The minimal possible $Q_{\min}$ is then calculated using this minimum BT, and the results are plotted in Fig. 4. The graph reveals that the minimal possible value of the adiabatic parameter in a sech/tanh pulse is $Q \simeq 1.6$, which is obtained

for $\upsilon = 1$, that is, for $A = B$. Thus, Figs. 3 and 4 justify our choice of constant r, and we shall limit ourselves henceforth to this choice.

Selecting $A = B \equiv r$, the modulation functions of the sech/tanh pulse are given by

$$\omega_1(t) = r\ \mathrm{sech}(\beta t)$$
$$\Delta\omega(t) = r\ \tanh(\beta t). \qquad [12]$$

The trajectory, a half circle, is identical with that of a CAP pulse though the rate of motion along the trajectory differs: As opposed to the CAP pulse, which sweeps the trajectory with a constant angular velocity (assuming $r = \mathrm{const}$), the sech/tanh pulse starts off very slowly and gathers speed as it advances along the trajectory. Its peak angular velocity is reached halfway through the pulse, when the tip angle is 90°. This scene is then played back symmetrically, so that the effective field vector slows down again. The adiabatic parameter manifests this behavior (cf. Eq. [10] with $\upsilon = 1$):

$$Q_{\mathrm{sech}}(t) = \frac{r}{|\dot{\theta}|} = \frac{r}{\beta}\cosh(\beta t). \qquad [13]$$

The adiabaticity at the beginning and end of the pulse is very good because of the slow motion of $\boldsymbol{\omega}_e$. The lowest value is obtained at the middle of the pulse, for $t = 0$, where

$$Q_{\mathrm{sech}}^{\min} = Q_{\mathrm{sech}}(0) = \frac{r}{\beta}. \qquad [14]$$

The dashed line in Fig. 1 shows the final M_z magnetization of a sech/tanh pulse for different pulse durations (cf. Eq. [20] in the Appendix). It can be appreciated that the behavior is similar to that of the CAP pulse with the same threshold duration.

Let us focus our attention on a sech/tanh pulse with minimal duration ($T = 2.7$ ms in our example). One might expect that this pulse exhibits adiabatic behavior similar to the threshold CAP pulse described previously. A puzzling situation, however, is revealed if we calculate the ratio between the minimal values of the adiabatic parameter of both pulses. We get, using Eqs. [7] and [14],

$$\frac{Q_{\mathrm{sech}}^{\min}}{Q_{\mathrm{CAP}}} = \frac{\Theta}{10.6} \simeq 0.3.$$

It is seen that the value the adiabatic parameter of the sech/tanh plunges to 30% of its value in an equal-duration CAP pulse. In particular, it was determined earlier that the minimal adiabatic parameter for a constant sweep rate CAP pulse is $Q_{\mathrm{CAP}} = q_0 = 5.4$. This was the lowest value that ensured tracking which, in turn, rendered inversion. An equal-duration sech/tanh pulse, on the other hand, accomplishes inversion with an adiabatic parameter as low as $Q_{\mathrm{sech}}^{\min} \simeq 1.6$ (cf. also Fig. 4).

This impression is further enhanced by examining the dashed line in Fig. 2. It is seen that the maximum angle subtended between the effective field vector $\boldsymbol{\omega}_e$ and the magnetization vector $\mathbf{M}$ during our threshold pulse is 44°, which is double the angle of the CAP pulse. It is difficult to associate such a large angle with ''adiabatic locking.''

It seems, in consequence, that the sech/tanh pulse is *not* performing adiabatic tracking. What, then, is the physics behind this behavior, that is, why is inversion achieved in spite of the nonadiabatic motion? Since the sech/tanh pulse allows us to perform faster inversion while violating the adiabatic condition, can this physical principle be exploited to design shorter pulses other than the sech/tanh pulse?

To answer these questions, it is instructive to examine the adiabatic pulse in a second-order rotating frame denoted SORF (*1, 6*). Figure 5a illustrates the frequency frame designated by the x', y', z' axes and the SORF designated by the x'', y'', z'' axes [nomenclature as in Ref. (*1*)]. The two frames coincide at the beginning of the pulse. The SORF rotates about the y'-axis during the pulse with the z''-axis aligned with the $\mathbf{B}_{\mathrm{eff}}$ vector. Therefore, in the SORF depicted in Fig. 5b, the $\mathbf{B}_{\mathrm{eff}}$ vector always points along the z''-axis. Since the SORF rotates with respect to the frequency frame at a rate of $(d\theta/dt)$, a ''virtual'' field of $-(d\theta/dt)$ must be added along the rotation axis $y' = y''$. As a result, the ''effective field'' in the SORF, designated $\mathbf{b}_{\mathrm{eff}}$ in Fig. 5b, is a sum of these two fields and is tilted away from the z''-axis by an angle of φ where, comparing with Eq. [2],

$$\cot\varphi = \frac{\|\boldsymbol{\omega}_e\|}{|\,d\theta/dt\,|} \equiv Q, \qquad [15]$$

that is, the cotangent of the tilt angle in the SORF is precisely the adiabatic parameter in the original frame. Fulfillment of the adiabatic condition [2] in the latter implies that $\cot\varphi \gg 1$, that is, $\varphi \simeq 0$. This, in turn, means that the ''virtual'' field vector $|\dot{\theta}|$ must be small. Observe that this vector is precisely the sweep rate of the original trajectory.

Let us demonstrate this point with respect to the CAP pulse of Eq. [5]. The z'' component is $r = \mathrm{const}$, whereas the y'' component is $\dot{\theta} = \Theta/T = \mathrm{const}$. Thus, the angle φ is fixed, with $\cot\varphi = r/\dot{\theta} \equiv Q_{\mathrm{CAP}}$. Adiabaticity is ensured by the condition $Q_{\mathrm{CAP}} \gg 1$ which, in turn, implies that the angle φ is small. In the SORF, the magnetization vector will precess around $\mathbf{b}_{\mathrm{eff}}$ with a fixed angle φ subtended between them. Therefore, the largest angle that may develop between the magnetization vector and the z'' axis is 2φ, which, by definition, is small. This explains adiabatic tracking of the CAP pulse using the second-order frame.

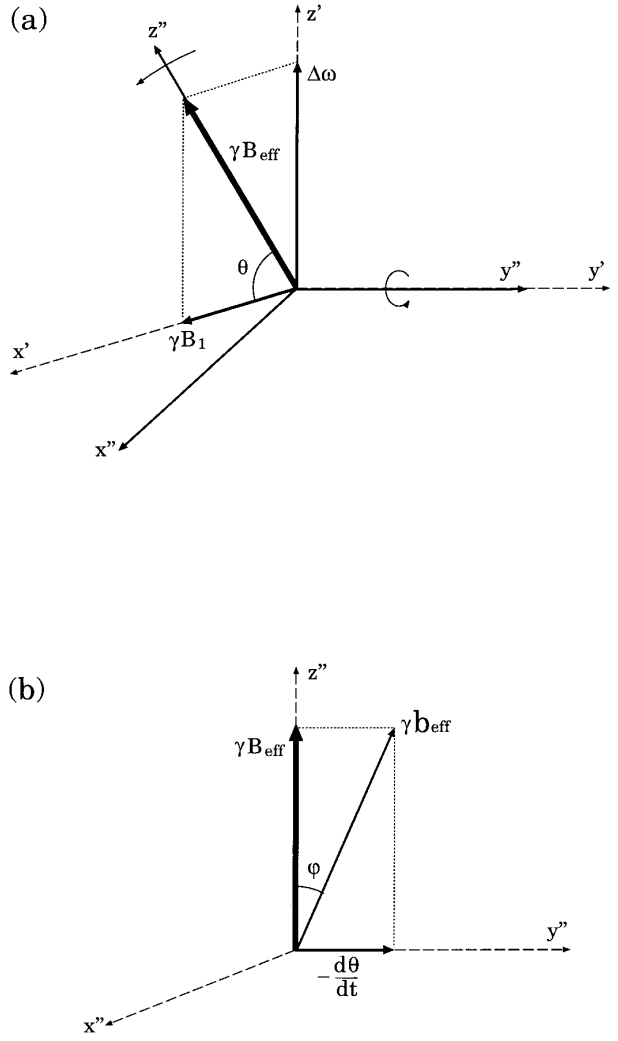

FIG. 5. (a) The frequency frame designated by the x', y', z' axes, and the second-order rotating frame (SORF) designated by the x'', y'', z'' axes. (b) The $\mathbf{b}_{\text{eff}}$ field in the SORF.

It is possible to increase the sweep rate $\dot{\theta}$ while still maintaining adiabaticity? The answer is in the affirmative as demonstrated by Fig. 6, which depicts the y''/z'' plane of the SORF. Increasing $\dot{\theta}$ tilts the $\mathbf{b}_{\text{eff}}$-vector away from the z'' axis, though the tip of this vector is confined to the horizontal line $z'' = r$. If this increase is performed slowly enough, the motion *in the SORF* will be adiabatic, causing the magnetization vector to follow the $\mathbf{b}_{\text{eff}}$ vector. Adiabaticity in the SORF is ensured by the condition

$$Q_2(t) = \frac{\|\gamma \mathbf{b}_{\text{eff}}\|}{|\dot{\varphi}|} \gg 1, \qquad [16]$$

where we designated the adiabatic parameter in the SORF by Q_2, the second-order adiabatic parameter, thereby referring to the adiabatic parameter Q in the original frequency frame as the first-order adiabatic parameter. Thus, the sweep rate $\dot{\theta}$ in the original frame may be increased to *any* value as long as condition [16] is obeyed. Moreover, this motion is definitely adiabatic although the adiabatic condition in the original frequency frame, Eq. [3], may be violated. In particular, for the sech/tanh pulse we obtain

$$Q_{2,\text{sech}}(t) = \frac{(r^2 \cosh^2(\beta t) + \beta^2)^{3/2}}{r\beta^2 |\cosh(\beta t)\sinh(\beta t)|}, \qquad [17]$$

the minimum of which is

$$Q_{2,\text{sech}}^{\min} = \frac{\alpha(2 + \alpha^2 + q)^{3/2}}{\sqrt{(1 + \alpha^2 + q)(1 + q)}}, \qquad [18]$$

where $\alpha \equiv r/\beta = Q_{\text{sech}}^{\min}$ and $q = \sqrt{1 + \alpha^2 + \alpha^4}$. It is easily seen that $Q_{2,\text{sech}}^{\min} > Q_{\text{sech}}^{\min}$, that is, the adiabaticity of the sech/tanh pulse is always better in the SORF. In particular, for our threshold pulse we have $Q_{\text{sech}}^{\min} = 1.6$, a nonadiabatic value, whereas $Q_{2,\text{sech}}^{\min} = 6.5$, which is by all means adiabatic. Moreover, the minimal possible ratio of the two parameters, $Q_{2,\text{sech}}^{\min}/Q_{\text{sech}}^{\min}$, is approximately 2.6. We conclude that the threshold sech/tanh pulse is indeed adiabatic in the SORF, whereas it is not in the original frequency frame.

What is the motion of the $\mathbf{b}_{\text{eff}}$ vector in the SORF during an adiabatic pulse? At the beginning and at the end of the pulse the $\mathbf{b}_{\text{eff}}$ vector must coincide with the $\mathbf{B}_{\text{eff}}$ vector, that is, be aligned with the z''-axis. In the middle of the pulse, $\mathbf{b}_{\text{eff}}$ is tilted away from the z''-axis by increasing $\dot{\theta}$, and is eventually returned to that axis by decreasing $\dot{\theta}$. When this is performed adiabatically the magnetization vector $\mathbf{M}$ follows $\mathbf{b}_{\text{eff}}$, both subtending an angle φ with the z''-axis, that is, with $\mathbf{B}_{\text{eff}}$. We described earlier what appeared to be nonadiabatic motion in the frequency frame where a large angle was spanned between $\mathbf{M}$ and $\mathbf{B}_{\text{eff}}$. It can now be understood that we were in fact observing adiabatic locking of $\mathbf{M}$ to the $\mathbf{b}_{\text{eff}}$ vector, and the large angle is actually the angle φ.

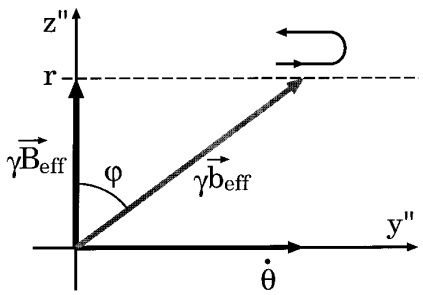

FIG. 6. The y''–z'' plane of the SORF.

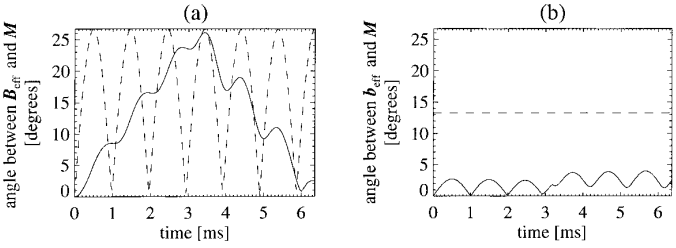

FIG. 7. (a) Frequency frame: the angle subtended between the effective field vector $\mathbf{B}_{\text{eff}}$ and the magnetization vector $\mathbf{M}$ during the 3π inversion pulses. (b) SORF: the angle subtended between the effective field vector $\mathbf{b}_{\text{eff}}$ and the magnetization vector $\mathbf{M}$. Linear pulse (solid line) and CAP pulse (dashed line). Amplitude is $r/2\pi = 1$ kHz and pulse duration is $T = 6.36$ ms.

Using the principles discussed here one can envisage other pulses besides the sech/tanh pulse which defy adiabaticity in the frequency frame but do behave adiabatically in the SORF. As a simple example, let us employ the same constant radius half-circle trajectory traced by the sech/tanh pulse. A pulse is then completely determined by the function $\dot{\theta}(t)$; for example, $\dot{\theta} = \beta\ \text{sech}(\beta t)$ for $t \in [-T/2, T/2]$ for the sech/tanh pulse. The simplest variant on this theme would be a pulse which varies its sweep rate linearly, viz.,

$$\dot{\theta} = g_0(T/2 - |t|),\ t \in [-T/2, T/2],$$

where $g_0 = 4\Theta/T^2$ (calculated so that $\Theta = \int_T \dot{\theta}\, dt$). The on-resonance performance of this pulse is similar to that of the sech/tanh inversion pulse, but can be utilized for large tip angles Θ (preferably integral multiples of π) as well as for inversion. In fact, the larger the tip angle, the more efficient the pulse is compared to a similar CAP pulse. Let us examine the first half of the pulse. We substitute $\tau = t - T/2$ so that $\dot{\theta}$ increases linearly with the new time variable τ, that is, $\dot{\theta} = g_0\tau$ for $\tau \in [0, T/2]$. The first-order adiabatic parameter is then given by

$$Q_{\text{LIN}} = \frac{rT^2}{4\Theta}\frac{1}{\tau} = \frac{r}{g_0}\frac{1}{\tau}, \qquad [19]$$

which shows that the adiabatic parameter decreases with time as $1/\tau$ and can diminish to very low values. The minimal values of the first- and second-order adiabatic parameters for the pulse are

$$Q_{\text{LIN}}^{\min} = \frac{rT}{2\Theta} \quad \text{and} \quad Q_{2,\text{LIN}}^{\min} = \frac{r^2T^2}{4\Theta},$$

and their ratio $Q_{2,\text{LIN}}^{\min}/Q_{\text{LIN}}^{\min} = rT/2$. For large tip angles $Q_{\text{LIN}}^{\min}$ may drop to very small values, whereas $Q_{2,\text{LIN}}^{\min}$ will still ensure adiabaticity.

As an example let us examine a $\Theta = 3\pi$ inversion pulse with amplitude $r/2\pi = 1$ kHz. We choose $g_0 = 0.932$ so that the resulting pulse duration is $T = 6.36$ ms. Figure 7 compares this pulse with a CAP pulse of equal duration and amplitude. Figure 7a depicts the angle subtended between the effective field vector $\mathbf{B}_{\text{eff}}$ and the magnetization vector $\mathbf{M}$ during the pulse as viewed from the frequency frame. It can be seen that for the CAP pulse the maximum angle is 26°—above the adiabatic threshold for a CAP pulse (21°). The adiabatic parameter for this pulse is $q_0 = 4.2$, which is well below the threshold value. It is not surprising, then, that the CAP pulse does not achieve full inversion. The linear pulse, on the other hand, performs the increase–decrease pattern discussed earlier. The maximal angle at mid-pulse is 26° but it decreases at the end of the pulse to less than 3°, which ensures robust inversion.

Figure 7b shows the angle between the effective field vector $\mathbf{b}_{\text{eff}}$ and the magnetization vector $\mathbf{M}$, both measured in the SORF. The maximal angle of 4° between the two vectors (vs 13° for the corresponding CAP pulse) confirms that excellent tracking is taking place in this frame.

In this paper we have gained new insight into the behavior of adiabatic pulses by switching into a second-order rotating frame of reference. It was shown that, although the pulse behaved nonadiabatically in the original frame, adiabaticity was preserved in the SORF. By transferring into the new frame of reference we gained a degree of freedom: We could liberate ourselves of the constraint on the angular velocity $\dot{\theta}$ (Eq. [3]); instead we obtained a limitation on $\dot{\varphi}$ (Eq. [16]) which was found to be less restrictive. Reexamining Fig. 6 we observe that the $\mathbf{b}_{\text{eff}}$ vector in this frame of reference is tilted away from the z''-axis at an angular rate of $\dot{\varphi}$. The same idea may be reapplied here: We can switch into a third-order rotating frame of reference which rotates about the x''-axis during the pulse with the z'''-axis aligned with the $\mathbf{b}_{\text{eff}}$ vector. This process could, in principle, be continued indefinitely, gaining a new degree of freedom by each switch. The analysis, though, becomes ever more complex.

In summary, a threshold sech/tanh pulse was shown to behave nonadiabatically in the frequency frame of reference. The adiabatic parameter plunged to low values which caused the ''adiabatic locking'' mechanism to break down. The puzzle was solved by switching into a second-order rotating frame of reference where the pulse was shown to obey the adiabatic condition. The degree of freedom that was gained during the switch could be used to design efficient adiabatic pulses with large tip angles.

APPENDIX

Expressions for $M_z(T)$ in sin/cos and sech/tanh Pulses

In this appendix expressions are derived for the final M_z magnetization on-resonance for the sin/cos and sech/tanh pulses with constant r.

For the sech/tanh pulse given by Eq. [12] we use Eq. [9] with $\upsilon = 1$. The result is

$$M_z^{\text{sech}} = -\tanh^2(\pi rT/21.2) + \text{sech}^2(\pi rT/21.2). \quad [20]$$

For the sin/cos (CAP) pulse given by Eq. [5], the analysis is best performed in the SORF (see Fig. 6) (*6*). Here, $\dot{\theta} = \pi/T$, $\tan\varphi = \pi/Tr$, and $\|\gamma \mathbf{b}_{\text{eff}}\| = \sqrt{r^2 + (\pi/T)^2}$. Our problem is to find the z'' component of the magnetization vector M_z at the time $t = T$. This vector is initially aligned with the z''-axis and precesses around the $\mathbf{b}_{\text{eff}}$ vector with a constant angular velocity $\Omega = \|\gamma \mathbf{b}_{\text{eff}}\|$ and with a fixed angle φ subtended between them. There is a well-known equation which describes this motion (see Ref. (*13*), p. 429, Eq. [14]), and the result is

$$M_z^{\text{CAP}} = -(\cos^2\varphi + \sin^2\varphi \cos \Omega T)$$
$$= -\frac{r^2T^2 + \pi^2\cos(\sqrt{\pi^2 + r^2T^2})}{\pi^2 + r^2T^2}. \quad [21]$$

Equations [20] and [21] were used to plot Fig. 1.

ACKNOWLEDGMENTS

The authors gratefully acknowledge valuable discussions with Dr. Shimon L. Panfil and with Maier Fenster.

REFERENCES

1. K. Ugurbil, M. Garwood, A. R. Rath, and M. R. Bendall, *J. Magn. Reson.* **78,** 472 (1988).
2. C. P. Slichter, ''Principles of Magnetic Resonance,'' 3rd Ed., Springer-Verlag, Berlin (1992).
3. C. J. Hardy, W. A. Edelstein, and D. Vatis, *J. Magn. Reson.* **66,** 470 (1986).
4. S. Conolly, D. Nishimura, and A. Macovski, *J. Magn. Reson.* **83,** 549 (1989).
5. M. S. Silver, R. I. Joseph, and D. I. Hoult, *J. Magn. Reson.* **59,** 347 (1984).
6. M. R. Bendall and D. T. Pegg, *J. Magn. Reson.* **67,** 376 (1986).
7. D. Rosenfeld, S. L. Panfil, and Y. Zur, *Phys. Rev. A* **54,** 2439 (1996).
8. J. Baum, R. Tycko, and A. Pines, *Phys. Rev. A* **32,** 3435 (1985).
9. K. Ugurbil, M. Garwood, and A. R. Rath, *J. Magn. Reson.* **80,** 448 (1988).
10. G. Town and D. Rosenfeld, *J. Magn. Reson.* **89,** 170 (1990).
11. M. S. Silver, R. I. Joseph, and D. I. Hoult, *Phys. Rev. A* **31,** 2753 (1985).
12. M. R. Bendall, *J. Magn. Reson. A* **116,** 46 (1995).
13. C. Cohen-Tannoudji, B. Diu, and F. Laloe, ''Quantum Mechanics,'' Vol. 1, Wiley–Interscience, New York (1977).